DSPACE

https://dspace.org/

Correlation Between Normalized Small Strain Shear Modulus and Shear Strength of FiberInduced MSW Fines

Parul Rawat; Supriya Mohanty

IRAN UNIV SCI & TECHNOL
https://hdl.handle.net/10539/42057
WOS

Downloaded from a DSpace repository. https://dspace.org/

International Journal of Civil Engineering (2024) 22:2091–2107
https://doi.org/10.1007/s40999-024-01014-8

RESEARCH PAPER

Correlation Between Normalized Small Strain Shear Modulus and Shear Strength of Fiber-Induced MSW Fines

Parul Rawat[1,2] · Supriya Mohanty[1]

Received: 12 June 2023 / Revised: 13 June 2024 / Accepted: 5 July 2024 / Published online: 22 July 2024
© The Author(s), under exclusive licence to the Iran University of Science and Technology 2024

Abstract

The primary objective of this investigation is to assess the potential reusability of aged, dumped waste found in landfills for its application as a bulk geomaterial. Owing to the inherent heterogeneity of municipal solid waste (MSW), comprehensively understanding its behaviour—be it physical, mechanical, or dynamic—presents a significant challenge. Laboratory-based studies serve as a pivotal means to gain insight into a material's behaviour before its practical implementation. The study focuses on examining the intricate strength characteristics of MSW fines (< 4.75 mm) and fiber-reinforced MSW fines (with varying fiber content ranging from 0 to 10%) using the bender element laboratory test. The bender element analysis facilitates the determination of shear wave velocity (V_s) values by measuring the disparity in time travel between transmitted and received waves. Comprehensive scrutiny encompasses the influence of diverse parameters, notably the excitation frequency of the wave (f), applied confining pressure (σ_c), relative compaction (R_c), fiber content (FC), and the saturation state. Notably, the study identified an optimal fiber content of 1% across different excitation frequencies and applied confining pressures, where V_s or normalized G_{max} values exhibited higher levels. Furthermore, the study involved fitting a cubic polynomial model and devising a generalized equation that correlates the normalized small strain modulus with the normalized shear strength for fiber-reinforced MSW fines. This equation serves as a valuable tool in understanding and predicting the material behaviour concerning small strain modulus and shear strength in fiber-reinforced MSW fines.

Keywords MSW fines · Fibers · Bender element test · Shear wave velocity · Small strain shear modulus

1 Introduction

Millions of tons of solid waste, treated or untreated, have been deposited every year in landfills, despite the development of advanced solid waste management techniques and major regulations. This becomes a need now to reutilize these landfills' waste and recover the land, either to reutilize it for other purposes or to accommodate the newly generated waste, as most of the old landfills have been exhausted. Landfills have become major structures to study for a few decades regarding their safety and stability under static and dynamic loadings due to the catastrophic disasters caused by landfill failures [1]. The high organic content and heterogeneity of landfill waste complicate the estimation of its engineering properties. The design, service, and management of landfills rely on understanding the thermo-hydro-mechanical (THM) properties of municipal solid waste (MSW), which influence the compressibility, strength, permeability, and overall stability of the landfills [2–4].

As compared to static behaviour, it has been more challenging to evaluate the dynamic behaviour of waste for landfill design due to its complex and heterogeneous material properties. There is a lot of research on the MSW (municipal solid waste) to study the effect of waste composition, particle size, unit weight, age, fiber content, etc.,

✉ Supriya Mohanty
supriya.civ@iitbhu.ac.in

Parul Rawat
parulrawat.rs.civ18@itbhu.ac.in

[1] Department of Civil Engineering, Indian Institute of Technology (BHU) Varanasi, Varanasi 221005, India

[2] School of Civil and Environmental Engineering, Faculty of Engineering and Built Environment, University of the Witwatersrand, Johannesburg 2050, South Africa

on the static geotechnical as well as on the dynamic properties (shear modulus and damping ratio) [5–17].

One of the relevant strength properties which are required for the seismic response analysis is G_{max} (small strain shear modulus), which has been indirectly computed from the shear wave velocity, (V_S), and the mass density of the material (ρ) relationship (as shown in Eq. 1 in subsequent sections). There are various in-situ methods used to determine the V_S of MSW, like Downhole sounding [18], Seismic refraction test [19], Seismic dilatometer test [20], Spectral analysis of surface waves method [21–25], Multichannel analysis of surface waves method, and Microtremor analysis method [25, 26]. To compute the dynamic properties of waste in the laboratory, the testing apparatus needs to be large to accommodate the large particle size, which is generally limited. So, to have reliable data most of the studies are carried out in fields to determine the V_S of MSW. The G_{max} obtained through V_S is generally associated with the shear strain of approximately 0.001% but, the in-situ techniques to evaluate the G_{max} of the MSW by measuring V_s with a small-strain range $> 0.001\%$ [27]. Few researchers have used some laboratory apparatus like bender element (BE) and resonant column (RC) to measure the G_{max} [27–29]. 15 large-scale cyclic simple shear tests installed with BE were conducted on reconstituted Tri-Cities landfill MSW specimens [29]. The test results demonstrated a strong dependence of unit weight and composition ratio on shear wave velocity and small strain shear modulus. Some research also tried to find the pulse velocities and elastic constants from the ultrasonic test for the MSW (below 4 mm) from the Mavallipura landfill site [30]. BE test on the MSW with varying fiber content from 0 to 6% concluded, that fiber content and confining pressure are of high importance for the evaluation of G_{max} [27]. On the other hand, several laboratory and field tests reported that laboratory-derived values are highly dependent on composition and time under specimen confinement [5].

The current study focuses on the reusability of excavated MSW fines, i.e., particles smaller than 4.75 mm, rather than the design and stability of the landfill itself. Approximately 60% of the waste collected in the present study was classified as MSW fines [31–33], even the past studies also validate this [34, 35]. These waste fines are generally used as soil cover, usually in the same landfills, but they can be used in bulk as construction or geomaterial once the material is determined to be suitable for application based on investigations [36–38]. Some of the research has also suggested landfill mine soil fraction can be used as fill material in reclamation projects, and restricted or unrestricted use in geotechnical projects depending on the organic content and chemical characterization of the fines [39, 40]. The investigation into the behavior of Municipal Solid Waste (MSW) fines and their potential utilization as bulk material in various applications is still in its nascent stages. The material's micro-level heterogeneity and unpredictable characteristics currently limit its practical application in different fields. Over the past few decades, the accumulation of vast waste in landfills, particularly in unsanitary landfills or dumpsites, has compelled researchers to focus on extracting and repurposing valuable materials from these sites. Given that the fine portion or soil-like material constitutes a significant proportion of these decomposed waste deposits, researchers recognize its potential as a substantial construction material. Notably, the Central Road Research Institute (CSRI) in New Delhi has researched employing waste from old landfills in Delhi as embankment fill material in road construction [36]. Moreover, the National Highways Authority of India (NHAI) has initiated the utilization of inert materials from such sources in select highway projects across India.

The dynamic perspective of the material has gained heightened significance, not only in its application within high seismic zones but also as a geomaterial in embankment or backfill, etc., where the particles undergo various vibrations due to nearby construction activities, traffic vibrations, and similar external factors. The particle range selected for the study makes it feasible to use the same sample size or apparatus as used for soil studies. Laboratory-based studies save time and money by predicting the behaviour of the materials under consideration before they are applied in the fields. The V_S of MSW fines and reinforced MSW fines with fibers was determined through the bender element apparatus in the laboratory. The fibers used were part of the waste and the impact on V_S was observed with the increased concentration of fibers in MSW fines. The details of the materials, bender element apparatus, and determination of shear wave velocity are discussed in the following sections.

2 Experimental Approach

2.1 Materials

The samples of waste were collected from two different sites. Site-1 was Ramana, Varanasi (Uttar Pradesh), India which was an open dump site. The samples were collected in bags from 4 to 5 points at an average depth of 1–2 m. The collected sample was further processed in the laboratory by drying and segregation and only the MSW fines (portion less than 4.75 mm) were used for extended studies [31, 32]. The second site (site- 2) was a waste-to-energy (WtE) plant located in Karsada, Varanasi (Uttar Pradesh), India. The 4 mm rejected sample, i.e., average size between 4 and 8 mm was collected from the plant. The

fibers were extracted from this waste by air-blowing method [31]. The location map of the sites is shown in Fig. 1. The considered samples of MSW fines and extracted fibers are shown in Fig. 2a and b. The detailed physical and geotechnical characterization has been discussed in the following result and discussion section.

2.2 Sample Preparation and Testing Methodology

The sample preparation procedure for the bender element test was the same as that of the triaxial test. Only the material used for sample preparation is MSW fines. The samples were prepared and tested at the required density. The samples were 100 mm in height and 50 mm in diameter and were compacted in four equal layers through the moist tamping method [41]. The samples prepared for fiber mixed/ reinforced MSW fines were the same as the unreinforced samples at a fixed density of 1.51 g/cc, i.e., the maximum dry density (MDD) of the MSW fines determined through the standard proctor test. The initial void ratio of the samples at a fixed density of 1.51 g/cc was observed to be 0.54 [42]. To check the effect of fiber content (FC), the considered MSW fines were mixed in different fiber proportions (0.5, 1, 2, 4, 8, and 10%). The fiber content was considered from the previously conducted study on the same material [31]. For the experiment, it was required to make groves on both sides of the sample so that

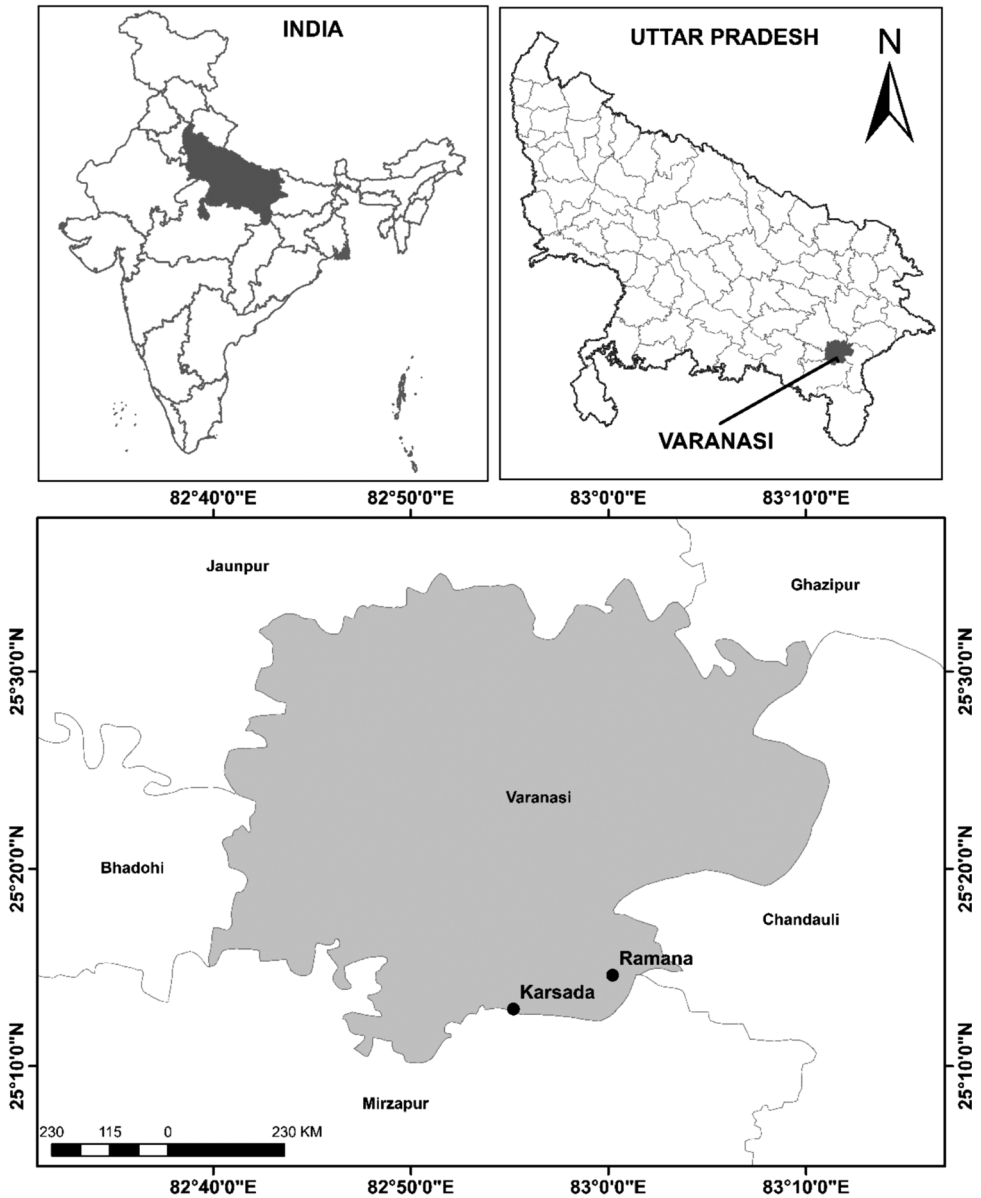


Fig. 1 Locations of waste collection sites

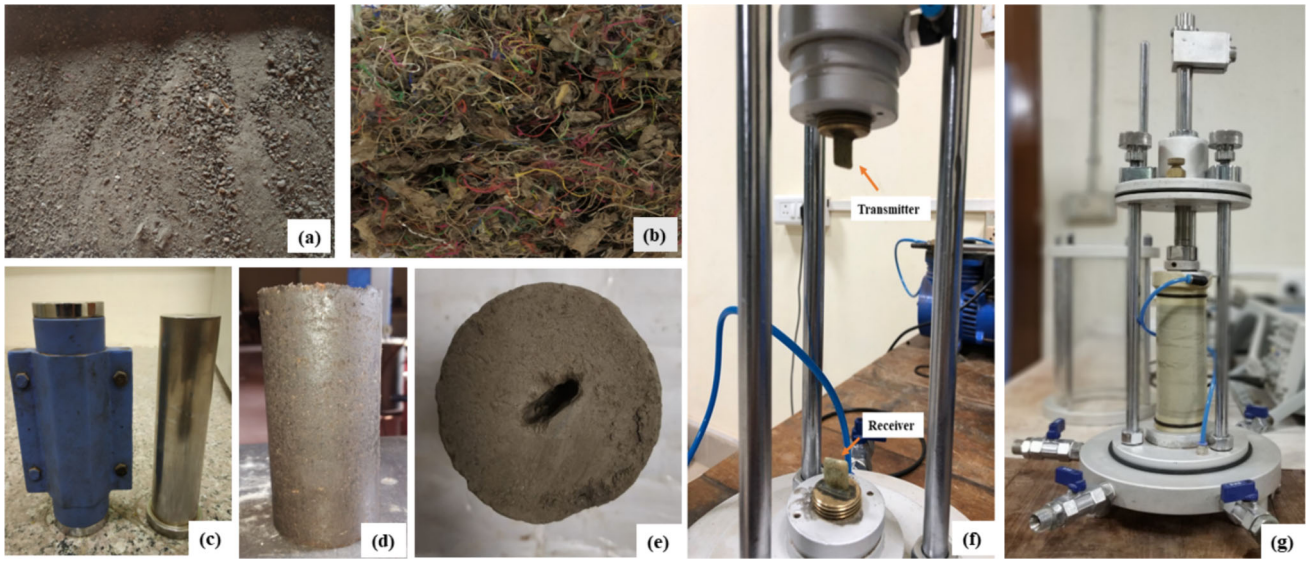


Fig. 2 **a** MSW fines sample, **b** Fibers sample segregated from waste, **c** Sampler, **d** prepared sample for bender analysis, **e** Prepared groove in the sample, **f** two bender elements fixed in triaxial cell, **g** mounted sample

the receiver and transmitter units of the bender element (Fig. 2(f)) could have better contact with the sample. The sample preparation mould, prepared sample, grove formed in the sample, and mounting of the sample in the cell have been shown in Fig. 2c, d, e, and g respectively.

The complete testing program can be seen in Fig. 3. The two sets of tests were carried out i.e., unreinforced and reinforced MSW fines with fibers. The unreinforced samples were tested for different relative compaction (R_c), i.e., 90, 92, 94, 96, 98, and 100% at different confining pressures (σ_c) of 0 to 200 kPa in the case of unsaturated samples and effective confining pressure (σ'_c) of 100 kPa for saturated samples. The considered frequency of wave or excitation frequency (f) for the unreinforced samples was in the range of 0.25 to 1.5 kHz. The reinforced samples were induced with the FC of 0.5 to 10% at a constant density and tested at a σ_c of 0 to 150 kPa in the case of unsaturated samples and σ'_c of 100 kPa for saturated samples. The f range was considered from 0.25 to 1.75 kHz. The bender element test was performed as ASTM D2845 [43].

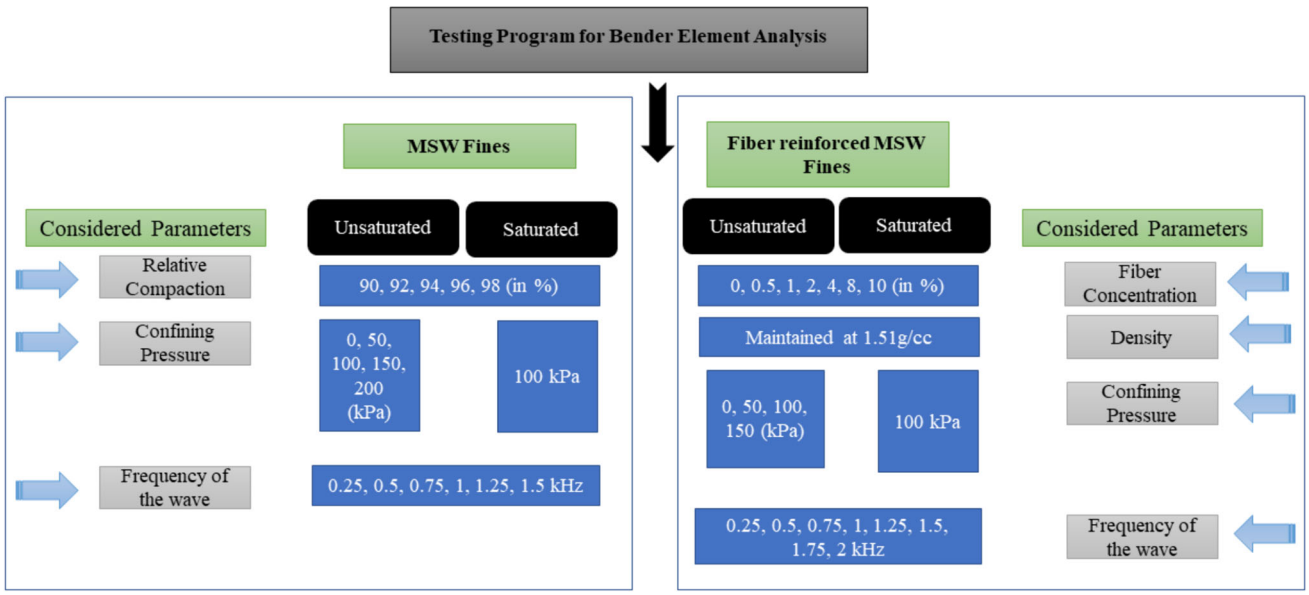


Fig. 3 Testing program for bender element analysis

2.3 Bender Element Apparatus

The bender element apparatus used for the study consists of four assemblies as shown in Fig. 4. It consists of one convertor unit or amplifier, one dual-channel wave function generator, one dual Channel high-performance digital oscilloscope, and one triaxial Cell with bender element for sample size 50 mm diameter. The two channels were attached from the convertor unit to the triaxial cell for transmitting and receiving the signals. The bender elements attached to the triaxial cell can be seen in Fig. 2(f). The upper end is the transmitter, where the waves enter the sample, and the lower end is the receiver. The waveform generator was connected to the amplifier's convertor unit. The waveform generator was used to provide input data, such as signal type (Sine, Triangular, Square, Random waveforms, and Ramp signal); frequency of wave; amplitude, etc. The generated input wave was received by the transmitter end of the triaxial cell, and waves traveled through the sample and were received by the receiver end before being sent back to the convertor unit. The digital oscilloscope was connected to the convertor unit and waveform generator, which displayed the input and output signals.

This apparatus possesses certain limitations. It is capable of solely measuring the material's shear wave velocity, whereas the bender-extender element apparatus has the capability to generate both P and S waves. The primary drawback of this apparatus pertains to the size of the bender element, approximately 1.2 cm, within the triaxial cell illustrated in Fig. 2(f). This larger size of the bender element poses challenges during sample preparation, often leading to multiple occurrences of sample breakage.

2.4 Determination of Shear Wave Velocity Through the Travel Time of Waves

The bender element test is based on the piezoelectric principle. The bender element test consists of a triaxial cell with a piezoelectric element attached to both ends. When excited with an electric voltage, these piezoelectric elements can convert electrical energy to mechanical energy. On the other end, another piezoelectric element receives the generated mechanical waves and converts them to an electric signal. The time lag between the generated input signal and the received output signal is recorded by the equipment. Because the distance traveled is constant, i.e., the tip-to-tip distance between the transmitter and receiver, which gives the velocity of the wave generated as a ratio of the travel length of the wave to travel time [44–46].

The most common and widely accepted method for determining the travel time in bender tests is the time domain (TD) analysis. A few approaches under TD analysis include the first start-to-start, first peak-to-peak, first trough-to-trough, and zero crossing of input–output waves. Although the time domain method yields reasonable results, it is seriously affected by the near-field effect (NFE) at low input frequencies [47, 48]. A transmitted shear wave is also often associated with a boundary-induced compressional wave, which can frequently cover up the shear wave at the receiver end which causes difficulty in travel time estimation. This phenomenon is called NFE [49, 50]. This effect can be minimized by adopting a suitable distance between the receiver and transmitter (L_{tt}) and the wavelength of the input signal (λ) [51]. It has been stated that the NFE was prominent if the L_{tt}/λ ratio value ranges from 0.24 to 4. The effects of NFE were greatly

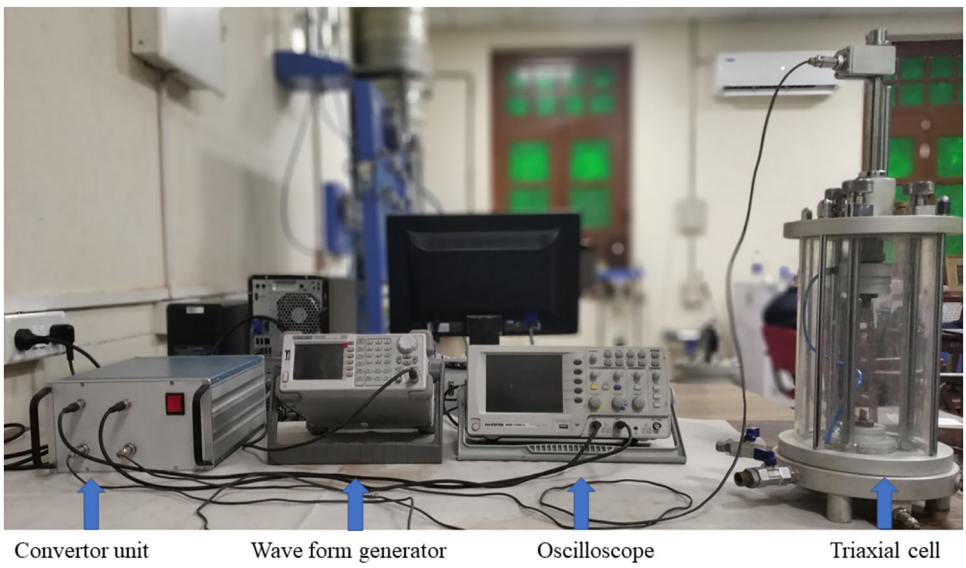


Fig. 4 Complete assembly of apparatus for bender element analysis

reduced for higher values, i.e., > 4 [52]. The time domain method is not much dependent on the frequency of the wave and does not explain the dispersive nature of the waves. The frequency domain analysis (FD) using Fourier transformation identifies the frequency components of the transmitted and received signals as cross-spectrum [53]. Even though the FD method yields lower velocities than the TD method, it gives a greater understanding of bender soil interaction behaviour [54]. Higher frequencies are preferable for FD analysis because they concentrate on the spectral frequency breakdown and phase shifts [55]. In addition, there is a mathematical method, known as the cross-correlation (CC) method which determines the similarity of input and output signals as a function of one signal's lag relative to the other. However, the CC method is regarded as a time-domain interpretation technique, even though calculations must be performed in the frequency domain [56]. It has been observed that at higher excitation frequencies, the velocity obtained from the cross-correlation technique is generally lower than that obtained from the peak-to-peak method [57].

In this study, the evaluation of shear velocity for the examined MSW and MSW-fiber composite was conducted using the time domain (TD) method, employing the peak-to-peak travel time estimation technique within the framework of the bender element test.

The V_s (shear wave velocity) obtained from the bender element test was used to find the small strain shear modulus (G_{max}) by applying the following expression (Eq. 1) [58]:

$$G_{max} = \rho V_s{}^2 = \rho \left(\frac{L_{tt}}{\Delta t}\right)^2 \quad (1)$$

where ρ = bulk mass density of the material (kg/m^3); V_s = velocity of the shear wave (m/sec), L_{tt} = travel length of the wave (tip to tip), and Δt is the travel time taken by the waves. The travel length of the wave is the effective length of the sample, i.e., the height of the sample (100 mm) minus the length of the bender elements from both sides. The length of each bender element was approximately 1.3 cm.

3 Results and Discussion

3.1 Geotechnical Characterization of MSW Fines and *Fiber*-Reinforced MSW Fines

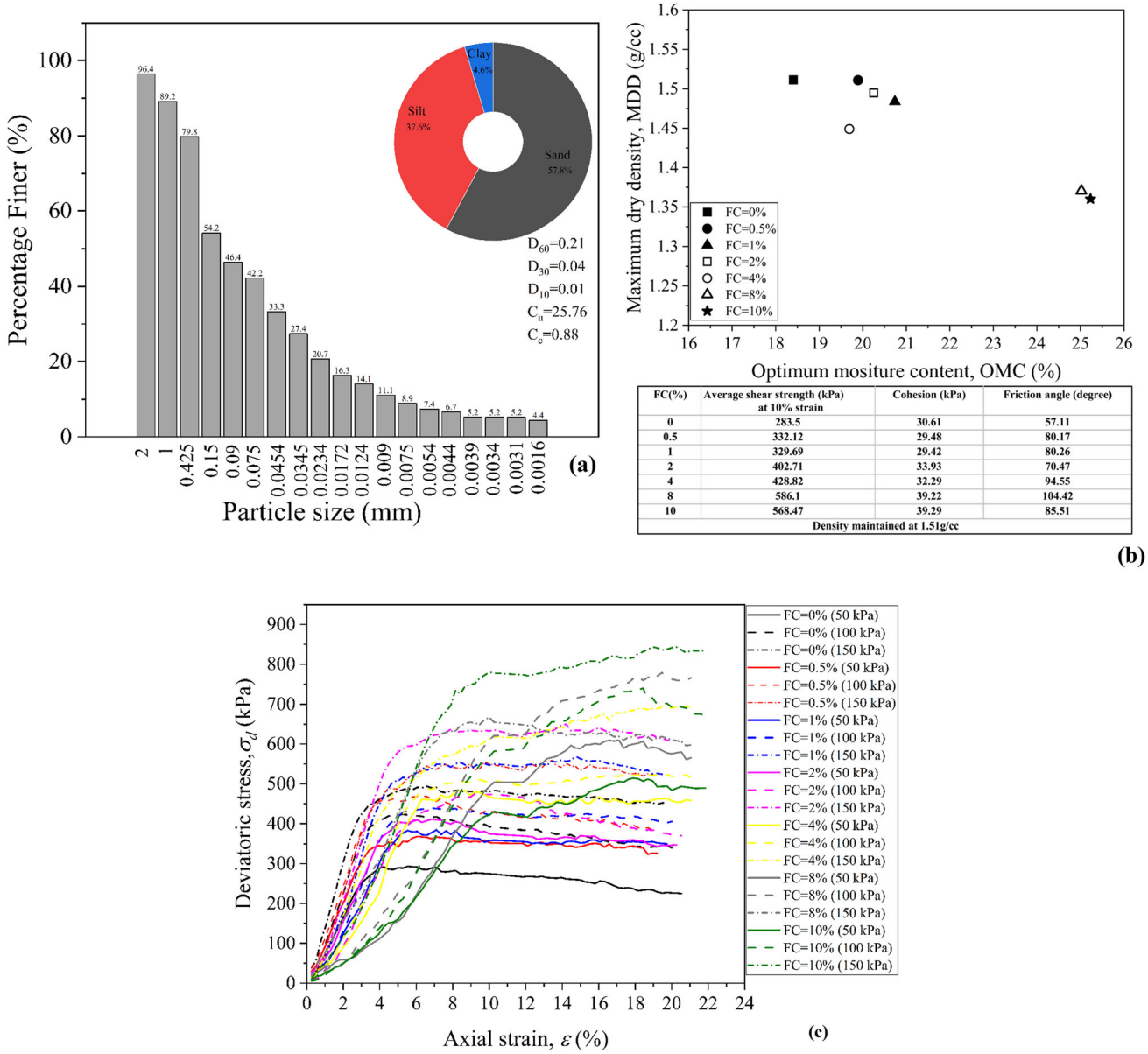
A detailed study (physical, chemical, geotechnical (static, and dynamic)) of the considered MSW fines has already been conducted in the past research [31, 32]. Approximately 60% of the waste collected from site 1 constituted MSW fines, characterized as a fraction smaller than 4.75 mm. The fundamental geotechnical assessment categorized these MSW fines as non-plastic silty sand, following the Unified Soil Classification System (USCS), with a specific gravity of 2.32. Details regarding the particle size distribution and physical characteristics of the MSW fines are presented in Fig. 5(a). Additionally, Fig. 5(b) illustrates the examination of density and strength variations of the MSW fines in correlation with the inclusion of fibers. These fibers have average length of 37 mm and low specific gravity of 0.82 [59]. The percentage increase of fiber inclusion due to its light weight reduces the dry density of the mixture whereas the average shear strength considered at 10% strain improves (when density is kept fixed at 1.51 g/cc) with FC up to 8%. The maximum percentage increase in average strength, in comparison to unreinforced MSW fines, reaches up to 106% with 8% fiber inclusion at a 10% strain. However, the enhancement in strength percentage appears modest at the initial fiber inclusion levels of 0.5% and 1%, approximately around 17% only. The same can be observed through stress–strain variation (for unsaturated undrained conditions and sample size of height 76 mm and diameter 38 mm) of the unreinforced and reinforced MSW fines at different confining pressures (50, 100, and 150 kPa) is shown in Fig. 5(c).

Based on the initial characterization, the MSW fines and the composite MSW fines-fiber mix show potential for utilization as fill material, such as backfill or embankment. However, further investigations and treatments are deemed necessary due to the presence of organic content. This organic content poses a potential risk for settlement and instability, requiring additional assessment and remedial measures before considering their practical application [31].

3.2 Bender Element Analysis

3.2.1 Consideration of Parameters for Bender Element Test

A total of five parameters were considered for the bender element study, i.e., R_c, σ_c, f, FC, and saturation which has already been discussed in the testing methodology. The study considered the time domain's first peak-to-peak analysis approach for the estimation of travel time as the peaks of the output signal were predominant and could be identified easily. However, more research is required to comment on which method works better for the geomaterials. The first start-to-start method was suggested as reliable by Georgetti and Rodrigues [60] and was used by some other researchers for waste and additive mix soils [58, 61]. However, it is sometimes difficult to identify the actual start point of the output signal. The input and output signals (sinusoidal) at different conditions with travel time can be seen in Fig. 6. It can be noticed that when the



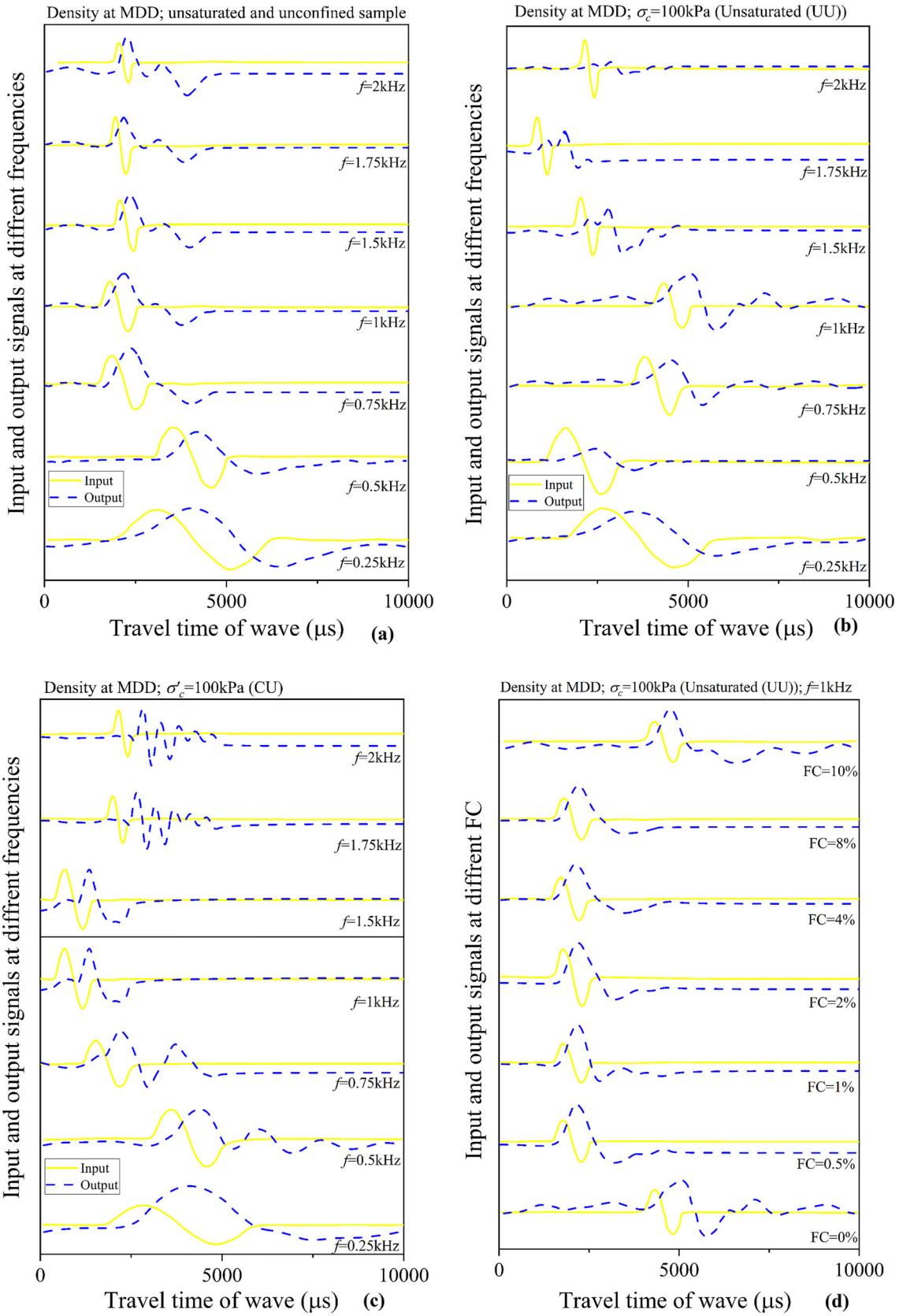
FC(%)	Average shear strength (kPa) at 10% strain	Cohesion (kPa)	Friction angle (degree)
0	283.5	30.61	57.11
0.5	332.12	29.48	80.17
1	329.69	29.42	80.26
2	402.71	33.93	70.47
4	428.82	32.29	94.55
8	586.1	39.22	104.42
10	568.47	39.29	85.51
Density maintained at 1.51g/cc			

Fig. 5 **a** Particle size characterization of MSW fines, **b** Compaction and strength characteristics, **c** Stress–strain variation of fiber-induced MSW fines. Source @ [31]

sample of MSW fines is unsaturated and unconfined (Fig. 6(a)) the output peaks (in blue) are predominant for all frequencies up to 2 kHz but as the sample is confined under σ_c = 100 kPa for UU (unconsolidated undrained) conditions (Fig. 6(b)) the first arrival output peak almost suppressed or vanished. This evaluates the first arrival output peaks at higher frequencies and confinement. When the MSW (fines) sample is saturated and the test was conducted under CU (consolidated undrained) conditions at σ'_c = 100 kPa (Fig. 6(b)), the predominant peaks can be seen again. A typical input–output signal graph at different FCs at a constant density (MDD) and f = 1 kHz is shown in Fig. 6(d).

3.2.2 Effect of Excitation Frequency (f) on V_s

The effect of the considered frequency range can be seen on the shear wave velocity (V_s) considering different FC and R_c (Fig. 7(a and b)). The V_s variation at every unconfined and confined (σ_c: 50, 100, and 150 kPa) condition for UU tests at different fiber content shows that V_s almost linearly varies with the excitation frequency of the wave (Fig. 7(a)). The concentration of fibers shows very minute effects on the V_s for every frequency. For the case of V_s variations with f for different R_c (Fig. 7(b)), the trends show slight improvement with the excitation frequency. For unconfined or low confined (50 kPa) cases the samples


Density at MDD; unsaturated and unconfined sample
Input and output signals at diffrent frequencies
f=2kHz
f=1.75kHz
f=1.5kHz
f=1kHz
f=0.75kHz
f=0.5kHz
f=0.25kHz
Input
Output
0
5000
10000
Travel time of wave (μs)
(a)
Density at MDD; σc=100kPa (Unsaturated (UU))
Input and output signals at diffrent frequencies
f=2kHz
f=1.75kHz
f=1.5kHz
f=1kHz
f=0.75kHz
f=0.5kHz
f=0.25kHz
Input
Output
0
5000
10000
Travel time of wave (μs)
(b)
Density at MDD; σ'c=100kPa (CU)
Input and output signals at diffrent frequencies
f=2kHz
f=1.75kHz
f=1.5kHz
f=1kHz
f=0.75kHz
f=0.5kHz
f=0.25kHz
Input
Output
0
5000
10000
Travel time of wave (μs)
(c)
Density at MDD; σc=100kPa (Unsaturated (UU)); f=1kHz
Input and output signals at diffrent FC
FC=10%
FC=8%
FC=4%
FC=2%
FC=1%
FC=0.5%
FC=0%
0
5000
10000
Travel time of wave (μs)
(d)

◀**Fig. 6** Input–output wave response for **a** unconfined unsaturated MSW fine sample at MDD, **b** unsaturated (UU) sample of MSW fine at σ_c (100 kPa), **c** saturated (UU) sample of MSW fine at σ'_c (100 kPa) at different excitation frequencies. **d** Input–output wave response at different FC for unsaturated MSW fine sample at σ_c (100 kPa) and f (1 kHz)

of lower R_c values show no improvement with the increase in excitation frequency. The improvements can be seen for higher σ_c i.e., above 50 kPa for all R_c values. The effect of R_c cannot be clarified from Fig. 7(b) and is discussed in the next section. Past researchers suggested the excitation frequencies for different types of soils for the sample aspect ratio of 2, i.e., silty sand (10 kHz) [62]; high plasticity clay (6 kHz) [55]; poorly graded sand (7 and 5 kHz) [47, 63]; and well-graded sand (10 kHz) [64]. The present MSW fines look like soils and are categorized as per the soil classification as silty sand, but the behavior of the material is quite different from that of the exact silty sand soil. This may be because of the heterogeneity of the material characteristics in the fines of the MSW.

3.2.3 Effect of Relative Compaction (R_c) on V_s

The differences in density or weight across various levels of relative compaction (R_c) did not exhibit distinct variations, making it challenging to discern clear trends in shear wave velocity (V_s) concerning R_c and draw definitive conclusions. However, noteworthy enhancements in V_s were observed, particularly at the lowest (90%) and highest (98%) R_c values, showcasing a remarkable improvement of over 100%, as detailed in Table 1. These improvements were particularly evident under unconfined conditions or at lower confinement levels (50 kPa).

However, as the applied confining pressure (σ_c) increased, the trends in V_s with varying R_c became less straightforward. While certain frequencies (0.75 and 1 kHz) displayed a marginal positive variation, there were

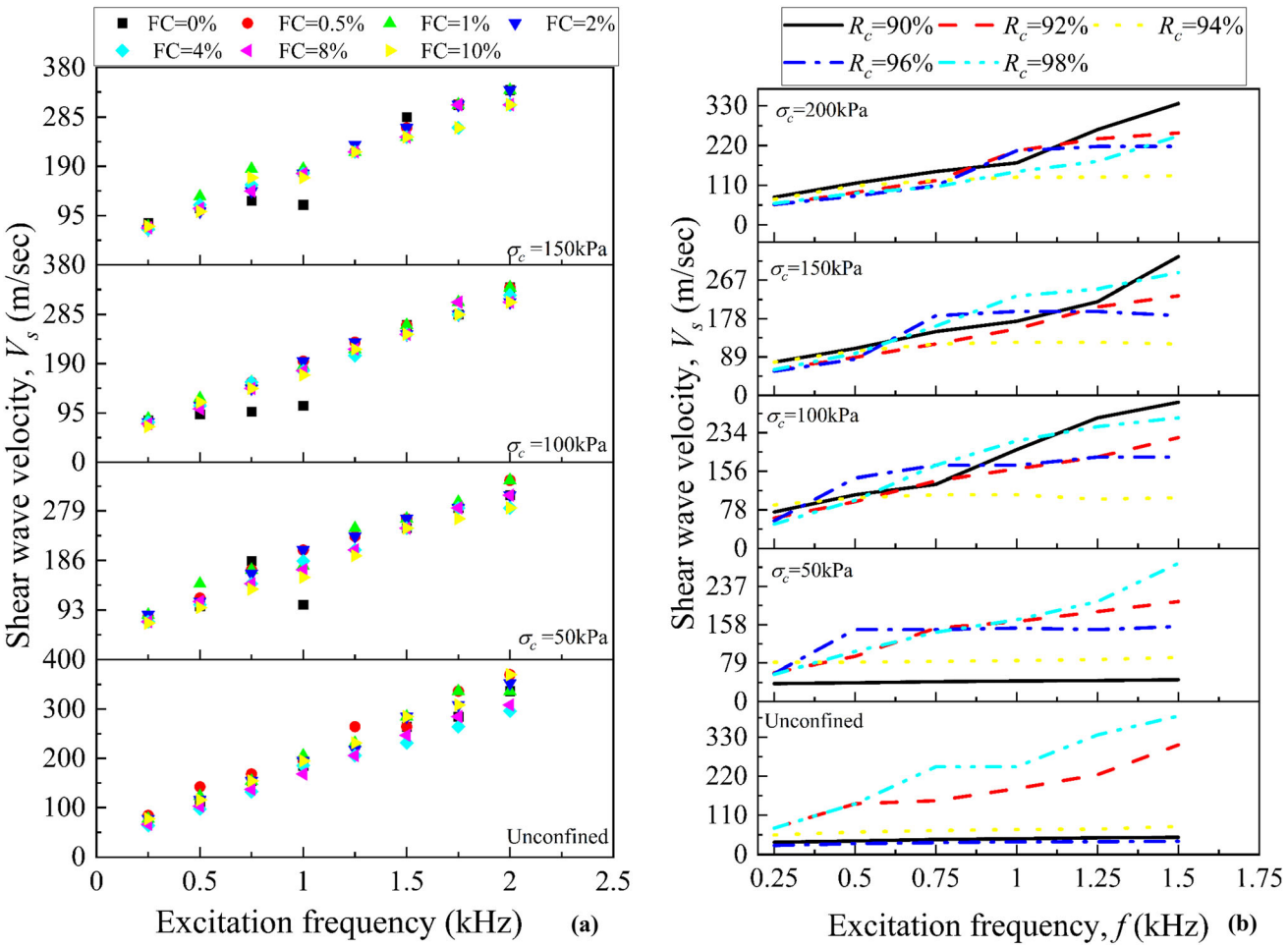


Fig. 7 Shear wave velocity (*Vs*) variations with excitation frequency (*f*) for **a** different fiber content (FC), **b** different relative compaction (R_c)

Table 1 R_c effect on V_s at different confining pressures and excitation frequencies

σ_c (kPa)	Unconfined		50 kPa		100 kPa		150 kPa	
R_c (%) / f (kHz)	90	98	90	98	90	98	90	98
0.25	34.26	74.00	37.00	56.06	74.00	49.33	77.08	59.68
0.5	37.75	142.31	38.94	102.78	108.82	97.37	108.82	97.37
0.75	42.045	246.67	41.11	142.31	129.82	168.18	148.00	160.87
1	44.047	246.67	42.53	168.18	200.00	217.65	172.09	231.25
1.25	46.84	336.36	43.53	205.56	264.29	246.67	217.65	246.67
1.5	48.05	389.47	45.12	284.62	296.00	264.28	321.74	284.62

*All the V_s values are in m/sec

V_s = Shear wave velocity; R_c = Relative compaction; σ_c = Confining pressure; f = Frequency

Testing conditions: Unconsolidated undrained (UU) without saturation

contrasting results observed with reduced V_s values at R_c (98%) for different frequencies (0.25, 0.5, and 1.5 kHz). The subtle alterations observed at higher confining pressures could potentially stem from variations in the density of the composite material initially set at lower relative compaction (R_c). These differences in density might contribute to the less pronounced outcomes observed in the study.

3.2.4 Effect of Confining Pressure (σ_c) on V_s

The influence of confining pressure on the shear wave velocity (V_s) of both unreinforced MSW fines and those reinforced with fibers across various FC appears negligible, as depicted in Fig. 8. While some fluctuations are noticeable in the unreinforced samples within the frequency range of 0.5 to 1 kHz, the introduction of fiber reinforcement tends to smoothen out these fluctuations. Table 1 indicates that at two distinct relative compactions (R_c), higher confining pressures (i.e., 100 and 150 kPa) have augmented the V_s in comparison to the unconfined or lower confinement (50 kPa) state. However, the extent of improvement shows minimal variation when transitioning from 100 to 150 kPa.

In Fig. 8, all samples were prepared at a constant density of 1.51 g/cc, which represents the maximum dry density (MDD) of the MSW fines. Consequently, any rearrangements of particles or alterations in density due to applied confining pressures might be challenging to observe. Nonetheless, in the case of R_c at 90%, where the density is lower than the MDD, such rearrangements could potentially occur owing to reduced compaction.

3.2.5 Effect of *Fiber* Content (FC) on V_s

To check the effect of FC on the V_s, two frequencies were considered i.e., 0.5 kHz (low) and 2 kHz (high) from the frequency range considered in this study. The analysis was made for four conditions (1) the samples were unsaturated and unconfined, (2) the samples were tested under unconsolidated undrained (UU) conditions at σ_c of 50, 100 and150 kPa, (3) the samples were tested under consolidated drained (CU) conditions at σ'_c of 100 kPa, and (4) unconfined sample after the third condition mentioned above. By comparing Fig. 9(a) for a frequency of 0.5 kHz and Fig. 9(b) for 2 kHz, the trends are almost the same, i.e., the maximum value of V_s can be seen for FC (1%) except for the condition (3) at 2 kHz frequency. Figure 9(a) also shows better results for unconfined or low confinement and after 4% fiber inclusions the trends change. There is no significant difference in V_s values was noticed with confinement for condition (2). However, in Fig. 9(b) the trends can be seen, i.e., higher V_s values at higher confinement with varying FC but the changes are not very significant. The unconfined sample (condition 1) of MSW with fiber reinforcement of 1% or 10% shows better performance at both the considered frequencies. To check the reinforcement effect on the maximum or small strain shear modulus (G_{max}), normalized values were considered, i.e., the ratio of G_R (reinforced shear modulus) to G_{UR} (unreinforced shear modulus). Typical plots were made for condition (2) in Fig. 9(c), and it can be seen for every case almost the peaks are at FC (1%) (except f:1 kHz & σ_c: 50 kPa considered as an anomaly). The better results can be seen for f (1 kHz), but the effect of increased confining is still unpredictable.

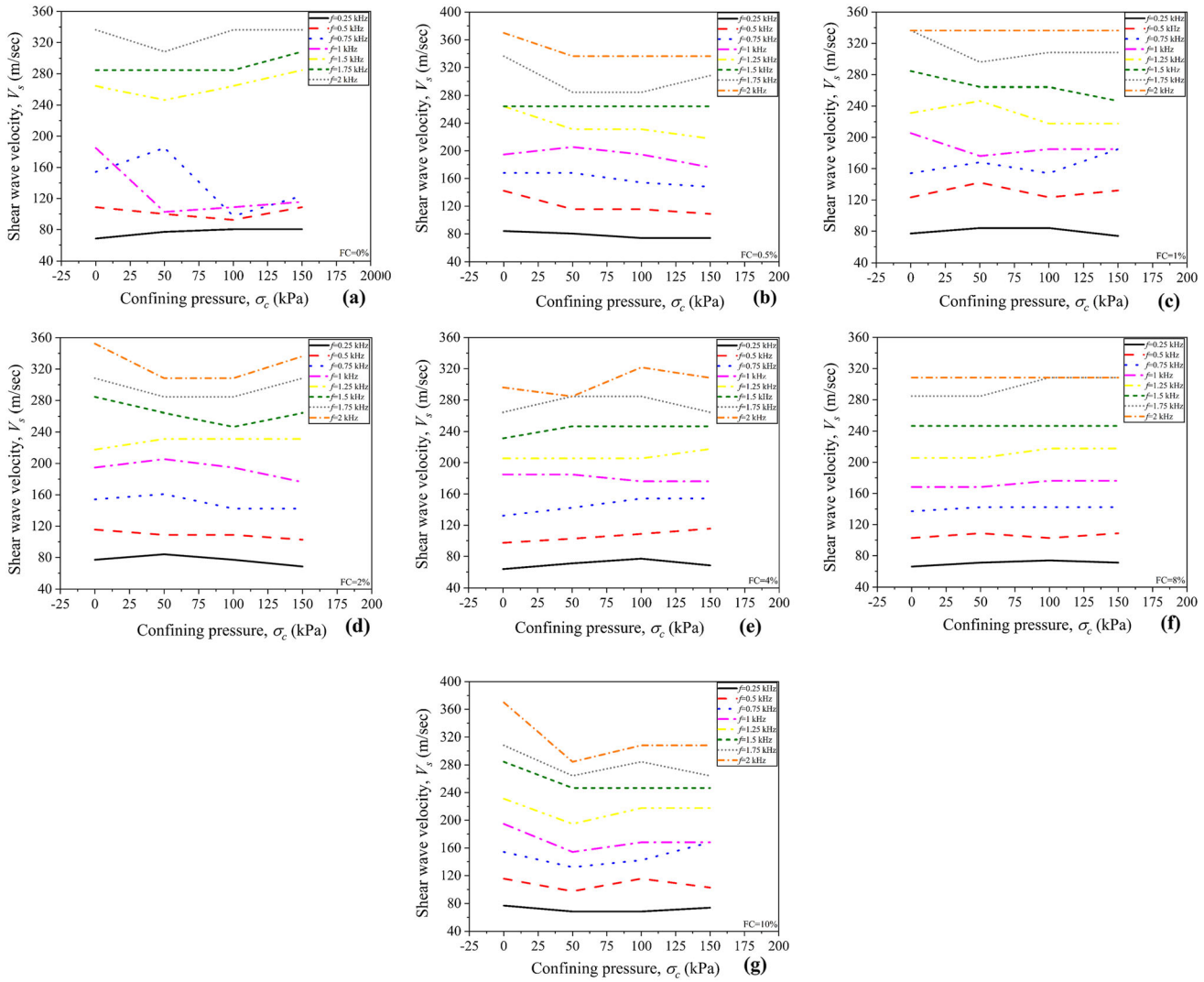


Fig. 8 Shear wave velocity (*Vs*) variation with confining pressure (σ_c) for different excitation frequencies (*f*) at fiber content (FC) of **a** 0%, **b** 0.5%, **c** 1%, **d** 2%, **e** 4%, **f** 8%, **g** 10%

3.2.6 Effect of Saturation on V_s

The saturation of the sample fills the voids with water which makes shear (S) waves take more time to travel through the medium because S waves could not pass through the liquid medium. This can also be seen in Fig. 9(a) and (b) for condition (3), as the sample gets saturated the V_s values drop compared to other conditions considered. The plot of V_s with the excitation frequency for UU and CU conditions shows unstable results (Fig. 10(a)). At low and high frequencies, the V_s is comparatively higher for UU conditions when the sample is in dry condition, but the difference is not very large. Comparing the two conditions at different R_c (Fig. 10(b)) a large variation can be seen especially at low densities and minimum at MDD. Sample prepared at MDD (maximum dry density), and OMC (optimum moisture content) are assumed to be almost saturated and likely to be less affected by the saturation and consolidation process.

4 Comparison of Present Study Results with Past Literature

The laboratory studies on the MSW are very limited, especially on the BE equipment. The major reason is the large particle size of the waste and the equipment size constrain the reliability of the data. The present study only considered the fine fraction, i.e., particle size less than 4.75 mm soil-like material of MSW. So, it can be compared with the other soil data. The study from the Mavallipura landfill site found that V_s and G_{max} for MSW samples less than 4 mm as 85, 95, 120 m/s and 5.05, 7.22, and 12.96 MPa respectively for the density of 7, 8, and 9

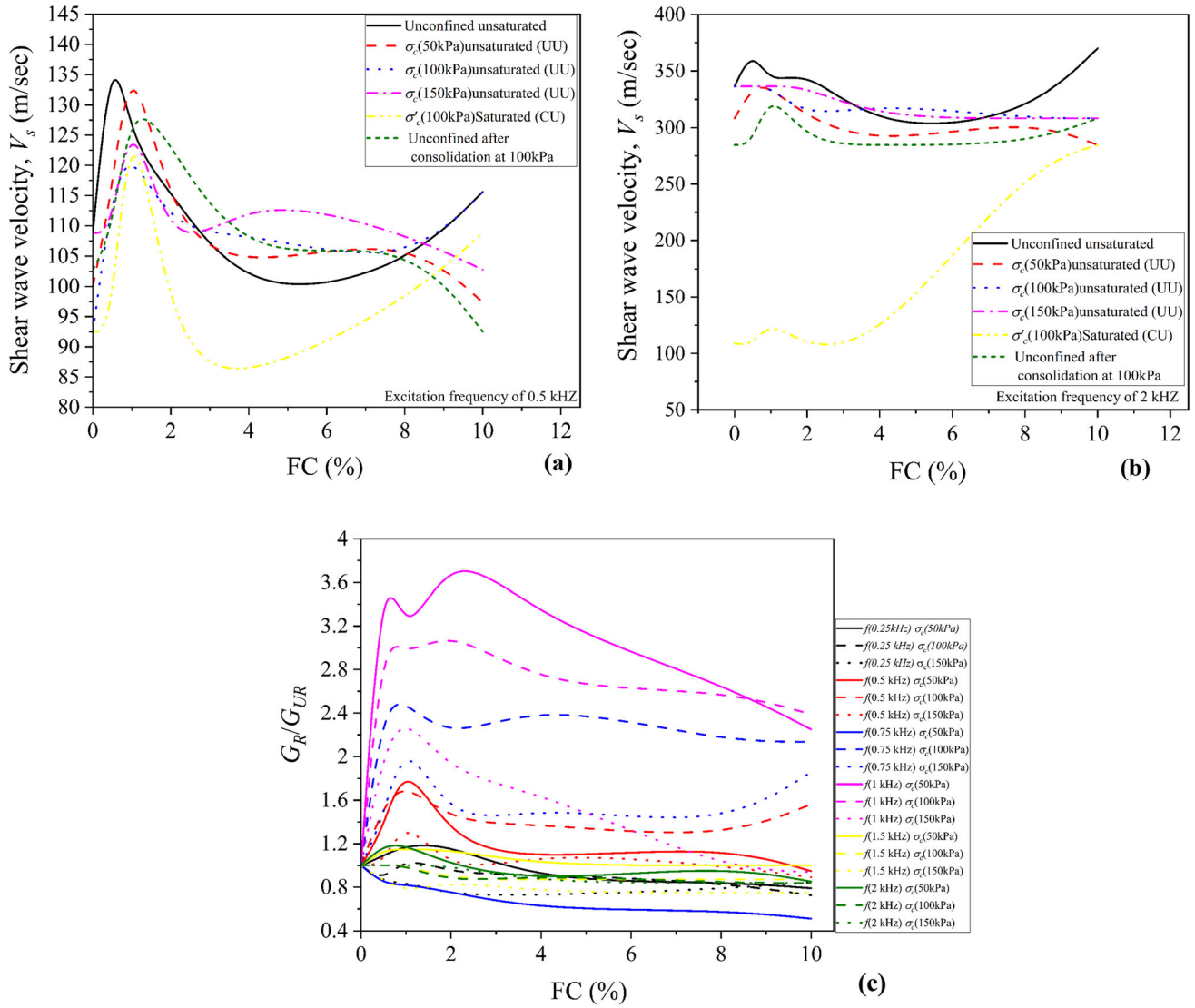


Fig. 9 Shear wave velocity (*Vs*) variation with fiber content (FC) at excitation frequency (*f*) of **a** 0.5 kHz, **b** 2 kHz. **c** Variation of G_R/G_{UR} ratio with FC for different excitation frequencies and confining pressure

kN/m^3 [30]. The data in the present study shows a great variation in V_s values as compared to the R_c as shown in Table 1. The major reasons for this much disparity in the results of MSW considered from the two sites are the (1) densities considered for the present study the MDD is about 15.1kN/m^3 (higher than considered in the above study); (2) the difference in the mechanical properties of the wastes; (3) heterogeneity at the micro level; (4) test conducted for analysis, as for the present study BE test was carried out whereas ultrasonic test was carried out for the Mavallipura landfill site waste.

Few past studies have been compared to the present fiber-induced MSW in Fig. 11. It can be observed that the inclusion of fibers (synthetic fibers) in sands generally reduces the G_{max} or the stiffness of the composite material. In the case of MSW, the inclusion of fiber contents reduces the arrival time of the received wave, because of the increased stiffness of the samples, while, at the same time, the bender receives low-voltage waves [27]. The observations are the same in the case of the present study (at an excitation frequency of 1 kHz) as the FC percentage increases the stiffness of the composite material improves up to a certain concentration in the unsaturated case and reduces for higher concentrations. The trends are reversed for the saturated and consolidated sample at 100 kPa. A plausible explanation for this observation could be attributed to the properties of the fibers utilized. The fibers employed in this research were a component of the waste and upon visual examination, exhibited characteristics closer to textile fabric than homogeneous plastic, presenting a predominantly heterogeneous nature. In contrast to most prior studies that focused on synthetic and

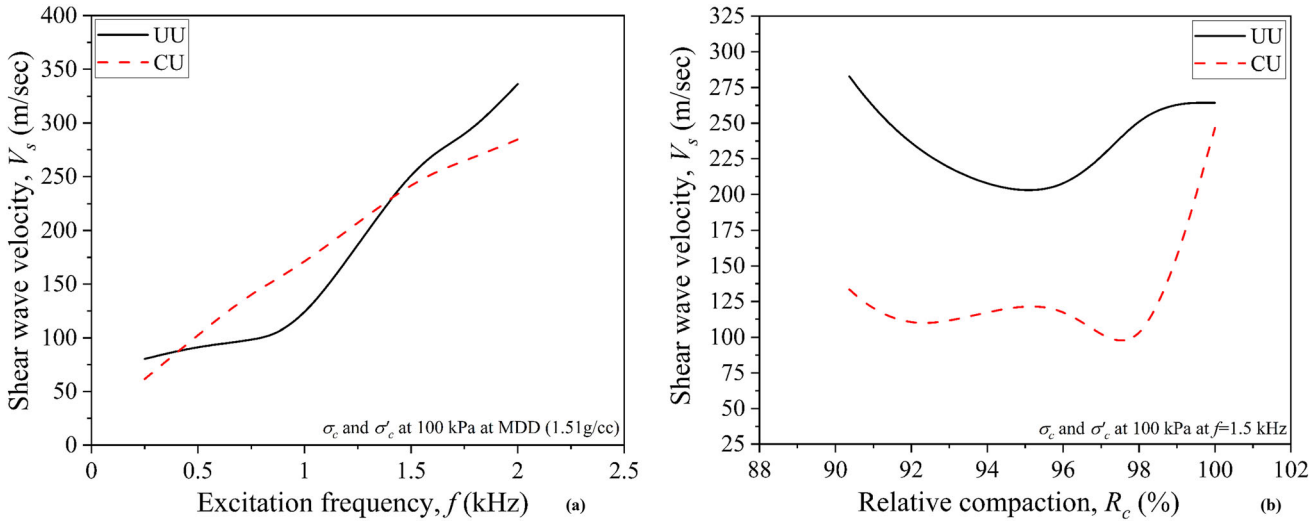


Fig. 10 Shear wave velocity (*Vs*) variation with **a** excitation frequency (*f*), **b** relative compaction (R_c) at *f* (1.5 kHz), for the MSW fine sample at MDD at UU and CU conditions

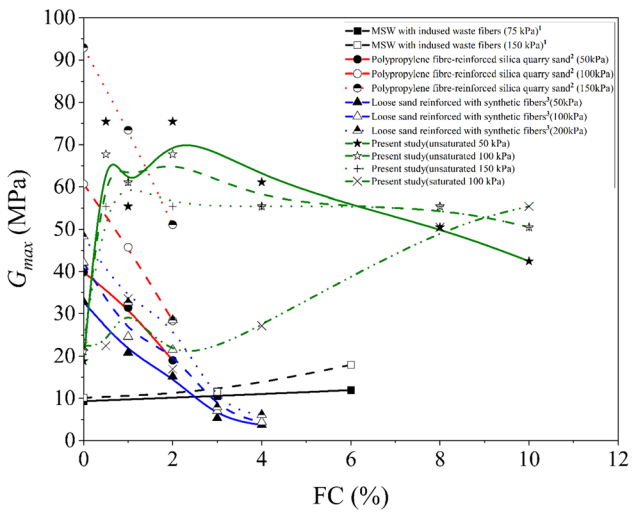


Fig. 11 Comparative past studies of small strain shear modulus (G_{max}) with fiber content (FC). (1-[27]; 2-[65]; 3-[66])

homogeneous fibers, these waste fibers display a notable capacity for water absorption, unlike synthetic fibers with negligible water-absorbing capabilities. Consequently, the waste fibers employed in this study tend to saturate with water, readily bonding with water molecules. As shear waves are impeded by water, the presence of water-saturated fibers obstructs the path of these waves, leading to a delay in their arrival time at designated points of detection.

5 Correlation Studies

All the test results were considered for the correlation study between the shear modulus (G_{max}) obtained from bender element analysis and the shear strength (τ) obtained from the triaxial test under UU (unconsolidated undrained) conditions considering unreinforced (UR) and fiber-reinforced (R) MSW fines. The G_{max} and τ values were normalized by taking the ratio of G_R/G_{UR} and τ_R/τ_{UR}, where G_R is the maximum shear modulus for fiber-reinforced MSW fines with different FC; G_{UR} is the maximum shear modulus for unreinforced MSW fines; τ_R is the maximum shear strength for fiber-reinforced MSW fines with different FC; τ_{UR} is maximum shear strength for fiber unreinforced MSW fines. Each data set consists of G_R/G_{UR} and τ_R/τ_{UR} values for every considered FC (0,0.5,1,2,4,8, and 10%) for different *f* (0.25,0.5,0.75,1, and 1.5 kHz) and σ_c (50, 100, and 150 kPa) (Fig. 12). The cubic polynomial non-linear model fits well with each data set and can be confirmed through the R^2 values which range from 0.7 to 0.99. Equation 2 defines the cubic polynomial model.

$$y = A + B * (x) + C * (x)^2 + D * (x)^3 \quad (2)$$

where y is the independent variable G_R/G_{UR} and x is dependent τ_R/τ_{UR} and A, B, C, and D are the constants. The values of the constants are defined in Table 2. Equation 2 can be written as Eq. 3.

$$G_R/G_{UR} = A + B * \left(\frac{\tau_R}{\tau_{UR}}\right) + C * \left(\frac{\tau_R}{\tau_{UR}}\right)^2 + D * \left(\frac{\tau_R}{\tau_{UR}}\right)^3 \quad (3)$$

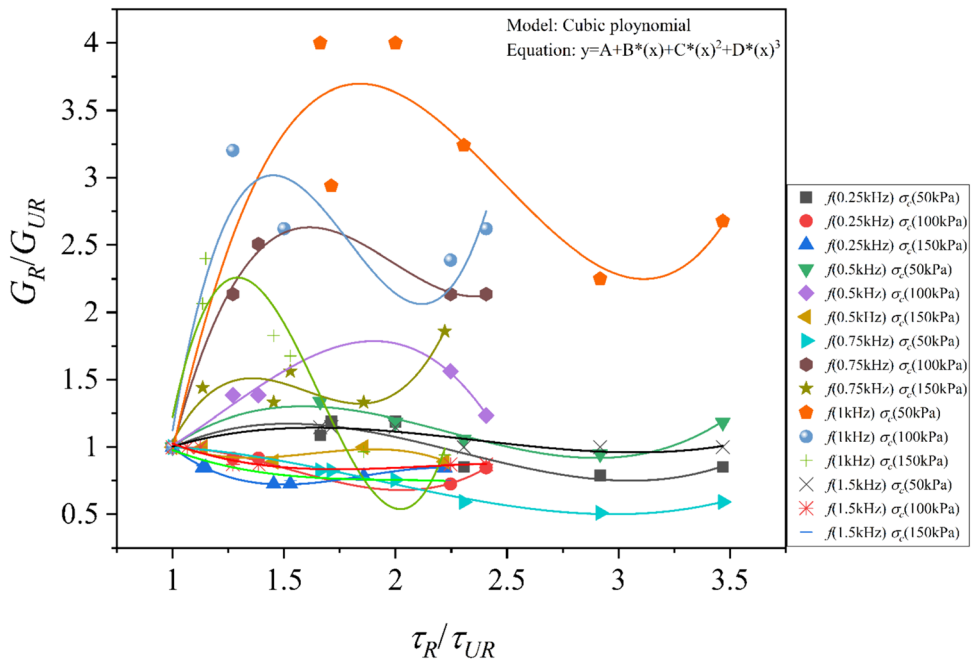


Fig. 12 Correlation between G_R/G_{UR} and σ_R/σ_{UR}

Table 2 Nonlinear fittings for the parameters A, B, C, and D used in the cubic polynomial model

S. No	f (kHz)	σ_c (kPa)	A	B	C	D	R^2
1	0.25	50	− 0.88 ± 0.89	3.25 ± 1.36	− 1.60 ± 0.66	0.23 ± 0.10	0.81
2	0.25	100	− 0.52 ± 0.92	3.61 ± 1.85	− 2.69 ± 1.19	0.59 ± 0.24	0.97
3	0.25	150	4.79 ± 0.22	− 7.03 ± 0.45	3.94 ± 0.28	− 0.71 ± 0.05	0.99
4	0.5	50	− 1.69 ± 0.41	4.62 ± 0.65	− 2.25 ± 0.32	0.33 ± 0.04	0.96
5	0.5	100	1.41 ± 2.6	− 2.67 ± 5.24	3.12 ± 3.39	− 0.84 ± 0.69	0.95
6	0.5	150	3.85 ± 2.42	− 5.71 ± 4.86	3.62 ± 3.12	− 0.74 ± 0.64	0.70
7	0.75	50	0.70 ± 0.28	0.79 ± 0.36	− 0.59 ± 0.17	0.10 ± 0.02	0.98
8	0.75	100	− 15.29 ± 2.32	28.80 ± 4.68	− 15.04 ± 3.02	2.5 ± 0.62	0.99
9	0.75	150	− 11.43 ± 5.52	25.29 ± 11.15	− 16.19 ± 7.20	3.37 ± 1.49	0.88
10	1	50	− 14.12 ± 4.36	24.11 ± 6.91	− 10.42 ± 3.38	1.40 ± 0.51	0.87
11	1	100	− 30.12 ± 18.56	59.22 ± 37.16	− 34.39 ± 23.78	6.42 ± 4.83	0.84
12	1	150	− 32.78 ± 11.01	68.95 ± 22.07	− 43.75 ± 14.20	8.80 ± 2.93	0.85
13	1.5	50	− 0.11 ± 0.38	1.86 ± 0.60	− 0.87 ± 0.29	0.12 ± 0.044	0.83
14	1.5	100	2.44 ± 0.93	− 2.39 ± 1.87	1.16 ± 1.21	− 0.18 ± 0.24	0.87
15	1.5	150	2.42 ± 2.21	− 2.46 ± 4.46	1.22 ± 2.88	− 0.20 ± 0.59	0.84

6 Conclusions

The escalating challenge of municipal solid waste (MSW) management is compounded by the unresolved issue of waste in old landfills. Extracting and repurposing over 60% of this waste, primarily composed of MSW fines or soil-like material, presents a viable solution. Dynamic characterization of this material, essential for its reuse as geomaterial, involves assessing shear wave velocity (V_s) and small strain shear modulus (G_{max}). Findings indicate a linear correlation between V_s and excitation frequency (f) up to 2 kHz, with notable improvements at higher

confining pressures (σ_c) above 100 kPa. While relative compaction (R_c) shows subtle effects on V_s comparing the lowest (90%) and highest (98%) R_c the improvements can be clear and optimal fiber content at 1% yields the highest values. Saturated conditions reduce V_s due to water-filled voids, and a cubic polynomial model correlates normalized small strain shear modulus and normalized shear strength. Despite the challenging nature of predicting V_s in the laboratory, especially for MSW fines with micro-level heterogeneity, this study sheds light on crucial factors influencing the dynamic behaviour of this soil-like material.

Funding This research did not receive any specific grant from funding agencies in the public, commercial, or not-for-profit sectors.

Declarations

Conflict of Interest The authors declare there are no competing interests.

References

1. Alidoust P, Kargar P, Goodarzi S, Keramati M, Moradi MH (2021) Laboratory-based assessment on similarities between dynamic behavior of MSW and clay. J Mater Cycles Waste Manag 23:622–643. https://doi.org/10.1007/S10163-020-01151-X
2. Yazdanpour B, Karimpour-Fard M, Sabermahani M, Machado SL (2024) Compression behavior of municipal solid waste in temperature-controlled isotropic condition. Geotech Test J 47:GTJ20230354
3. Khaleghi M, Heshmati AAR, Karimpour-Fard M, Machado SL (2024) Thermal efects on the compressibility and permeability of municipal solid waste landfills. Int J Environ Sci Technol 21:73–90
4. Khaleghi M, Karimpour-Fard M, Heshmati AA, Machado SL (2023) Thermo–hydro–mechanical response of MSW in a modified large oedometer apparatus. Int J Geomech 23:04022310
5. Zekkos D (2005) Evaluation of static and dynamic properties of municipal solid waste. University of California, Berkeley
6. Towhata I, Kawano Y, Yonai Y, Koelsh F, Koelsch F (2004) Laboratory tests on dynamic properties of municipal wastes. 11th Conf. Soil Dyn. Earthq. Eng. 3rd Int Conf Earthq Geotech Eng, pp 688–693.
7. Naveen B, Sitharam T, Sivapullaiah P (2019) Seismic behavior and dynamic site response of municipal solid waste landfill in India. In: Sitharam TG, Vinod JS (eds) Recent challenges and advances in geotechnical earthquake engineering. IGI Global, pp 168–196
8. Magnanelli E, Tranås O, Carlsson P, Mosby J, Becidan M (2020) Dynamic modeling of municipal solid waste incineration. Energy 209:118426
9. Feng S, Chang J, Chen H (2018) Seismic analysis of landfill considering the effect of GM-GCL interface within liner. Soil Dyn Earthq Eng 107:152–163
10. Matasovic N, Zekkos D, Sahadewa A, Carlson CP (2018) In situ testing for evaluation of modulus reduction and damping of municipal solid waste at a hazardous waste landfill. InGeotechnical Earthquake Engineering and Soil Dynamics V Slope Stab. Landslides, Lab. Testing, Situ Test, Reston: American Society of Civil Engineers (ASCE), pp. 452–60. https://doi.org/10.1061/9780784481486.047.
11. Karimpour-Fard M, Alaie R, Souf GR, Machado SL, Foumani ER, Moghadam RRM (2021) Laboratory study on dynamic properties of municipal solid waste in saravan landfill. Iran Int J Civ Eng 19:861–879
12. Karimpour-Fard M (2019) Rehabilitation of Saravan dumpsite in Rasht, Iran: geotechnical characterization of municipal solid waste. Int J Environ Sci Technol 16:4419–4436. https://doi.org/10.1007/s13762-018-1847-z
13. Keramati M, Shariatmadari N, Karimpour-Fard M, Saeedanezhad A, Alidoust P (2019) Effect of aging on dynamic properties of municipal solid waste: a case study of Kahrizak Landfill, Tehran. Iran Sci Iran 26:1077–1088
14. Keramati M, Shariatmadari N, Karimpour-Fard M, Nabizadeh SM (2016) Dynamic behaviour of MSW materials under cyclic triaxial testing: a case of Kahrizak landfill, Tehran. Iran Iran J Sci Technol Trans Civ Eng 40:75–83
15. Shariatmadari N, Asadi M, Karimpour-Fard M (2017) Investigation of fiber effect on the mechanical behavior of municipal solid waste by different shearing test apparatuses. Int J Environ Sci Technol 14:2239–2248
16. Asadi M, Shariatmadari N, Karimpour-Fard M, Noorzad A (2017) Validation of hyperbolic model by the results of triaxial and direct shear tests of municipal solid waste. Geotech Geol Eng 35:2003–2015
17. Karimpour-Fard M, Machado S (2012) Deformation characteristics of MSW materials. Electron J Geotech Eng 17:2009–2024
18. Houston W, Houston S, Liu J, Elsayed A, Sanders C (1995) In-situ testing methods for dynamic properties of MSW landfills. In: Yegian M, Liam Finn W, editors. In: Proceedings Geotech. Eng. Div. ASCE Conjunction with ASCE Conv., Reston, VA: ASCE, pp. 73–82
19. Kholmatov K, Khashimova D, Wu W (2007) Geophysical site investigation of landfill in seismically active region of Tashkent, Uzbekistan. Environmental science and technology, global network for environmental science and technology (Global-NEST), Athens, Greece: pp. 1326–33
20. Castelli F, Lentini V, Maugeri M (2012) Static and dynamic waste characterization. In: Servicios R, (Eds) In Proc., 5th Eur. Geosynth. Congr. EUROGEO, Spain, pp. 105–10
21. Kavazanjian EJ, Matasovic N, Stokoe KI, Bray J (1996) In situ shear wave velocity of solid waste from surface wave measurements. In: Proceedings 2nd Int. Congr. Environ. Geotech. Balkema, Rotterdam, Netherlands, pp. 97–102
22. Cuellar V, Monte J, Valerio J (1998) Static and dynamic elastic moduli for waste landfills. 3rd Int. Congr. Environ. Geotech. Vol. 1, Balkema, Amsterdam, Netherlands, pp. 325–9
23. Matasovic N, Kavazanjian JE (2006) Seismic response of a composite landfill cover. J Geotech Geoenviron Eng 132:448–455. https://doi.org/10.1061/ASCE1090-02412006132:4448
24. Zekkos D, Sahadewa A, Woods R, Stokoe K (2014) Development of model for shear-wave velocity of municipal solid waste. J Geotech Geoenviron Eng 140:00401303. https://doi.org/10.1061/(ASCE)GT.1943-5606.0001017
25. Ramaiah B. Static and dynamic slope stability assessment of municipal solid waste dump sites in Delhi. Indian Institute of Technology, New Delhi, India, 2014.
26. Sahadewa A, Zekkos D, Lobbestael A, Woods R (2011) Shear wave velocity of municipal solid waste in Michigan landfills. 14th Pan-American Conf. Soil Mech. Geotech. Eng. 64th Can.

Geotech. Conf. Geo-Innovation Addressing Glob. Challenges, Richmond, BC, Canada: Canadian Geotechnical Society
27. Alidoust P, Keramati M, Shariatmadari N (2018) Laboratory studies on effect of fiber content on dynamic characteristics of municipal solid waste. Waste Manag 76:126–137. https://doi.org/10.1016/j.wasman.2018.02.038
28. Hossain M, Haque M, Hoyos L (2010) Dynamic properties of municipal solid waste in bioreactor landfills with degradation. Geotech Geol Eng 28:391–403. https://doi.org/10.1007/S10706-009-9299-3
29. Yuan P, Kavazanjian JE, Chen W, Seo B (2011) Compositional effects on the dynamic properties of municipal solid waste. Waste Manag 31:2380–2390
30. Naveen B (2018) Measurement of static and dynamic properties of municipal solid waste at Mavallipura landfill site. India Int J Geo-Engineering 9:1–22. https://doi.org/10.1186/S40703-018-0088-9
31. Rawat P, Mohanty S (2021) Experimental investigation on MSW fine mixed with fibers: fiber reinforced waste. J Hazard, Toxic, Radioact Waste 25:04021009. https://doi.org/10.1061/(ASCE)HZ.2153-5515.0000609
32. Rawat P, Mohanty S (2022) Parametric study on dynamic characterization of municipal solid waste fine fractions for geotechnical purpose. J Hazard, Toxic, Radioact Waste 26:04021047. https://doi.org/10.1061/(ASCE)HZ.2153-5515.0000659
33. Rawat P, Mohanty S (2023) Static and dynamic loading effects on the strength characteristic of municipal solid waste (MSW) fines reinforced with geosynthetics. Sādhanā 49:1–15
34. Mönkäre T, Palmroth M, Rintala J (2016) Characterization of fine fraction mined from two Finnish landfills. Waste Manag 47:34–39
35. Somani M, Datta M, Ramana GV, Sreekrishnan T (2018) Investigations on fine fraction of aged municipal solid waste recovered through landfill mining: case study of three dumpsites from India. Waste Manag Res 36:744–755. https://doi.org/10.1177/0734242X18782393
36. Havangi VG, Sinha AK, Parvathi G, Chandra S (2017) Municipal solid waste in road embankment construction—a case study. J Indian Roads Congr 78–90
37. Rawat P, Mohanty S (2021) Utilization of municipal solid waste as backfill material. Proceedings of the Indian Geotechnical Conference 2019: IGC-2019. Springer, Singapore, pp 49–62. https://doi.org/10.1007/978-981-33-6370-0_5
38. Singh A, Chandel M (2022) Valorization of fine fraction from legacy waste as fired bricks: a step towards circular economy. J Clean Prod 331:129918
39. Datta M, Gupta G, Somani M (2021) Geoenvironmental considerations for bulk reuse of MSW residues from old dumps and WTE plants in geotechnical applications. Indian Geotech J 51:63–83. https://doi.org/10.1007/S40098-020-00491-7
40. Chandana N, Goli VSNS, Mohammad A, Singh DN (2021) Characterization and utilization of landfill-mined-soil-like-fractions (LFMSF) for sustainable development: a critical appraisal. Waste and Biomass Valor 12:641–662. https://doi.org/10.1007/S12649-020-01052-Y
41. Degregorio VB (1990) Loading systems, sample preparation, and liquefaction. J Geotech Eng 116:805–821. https://doi.org/10.1061/(ASCE)0733-9410(1990)116:5(805)
42. Rawat P, Mohanty S (2022) One-dimensional compressibility study on fiber-reinforced municipal solid waste (MSW Fines). Indian Geotech J. https://doi.org/10.1007/S40098-022-00679-Z/TABLES/3
43. ASTM-D2845 (2000) Standard test method for laboratory determination of pulse velocities ultrasonic elastic constants of rock. United States, Philadelphia
44. Kang X, Kang GC, Bate B (2014) Shear wave velocity anisotropy of kaolinite using a floating wall consolidometer-type bender element testing system. Geotech Test J 37:869–883. https://doi.org/10.1520/GTJ20120205
45. Camacho-Tauta J, Reyes-Ortiz O, Jiménez ÁJ (2013) Comparison between resonant-column and bender element tests on three types of soils. Dyna 80:163–172
46. Hoyos L, Suescún-Florez E, Puppala A (2015) Stiffness of intermediate unsaturated soil from simultaneous suction-controlled resonant column and bender element testing. Eng Geol 188:10–28
47. Sanchez-Salinero I, Roesset J, Stokoe I, Kenneth H (1986) Analytical studies of body wave propagation and attenuation
48. Lee JS, Fernandez AL, Santamarina JC (2005) S-wave velocity tomography: small-scale laboratory application. Geotech Test J 28:336–344. https://doi.org/10.1520/GTJ12638
49. Arroyo M, Wood DM, Greening P, Medina L, Rio J (2006) Effects of sample size on bender-based axial G0 measurements. Géotechnique 56:39–52. https://doi.org/10.1680/geot.2006.56.1.39
50. Brignoli EG, Gotti M, Stokoe KH (1996) Measurement of shear waves in laboratory specimens by means of piezoelectric transducers. Geotech Test J 19:384–397. https://doi.org/10.1520/GTJ10716J
51. Mancuso C, Simonelli A, Vinale F (1989) Numerical analysis of in-situ S-wave measurements. Congrès Int. mécanique des sols des Trav. Fond, Rio de Janeiro, pp 277–280
52. Jovicic V, Coop M, Simic M (1996) Objective criteria for determining Gmax from bender element. Geotechnique 46:357–362. https://doi.org/10.1680/GEOT.1996.46.2.357
53. Nash D, Sukolrat J, Greening P, Benahmed N (2007) Comparison of shear wave velocity measurements in a soft clay specimen using time and frequency domain techniques. Riv Ital Di Geotec 25:56–68
54. Ingale R, Patel A, Mandal A (2017) Performance analysis of piezoceramic elements in soil: a review. Sens Actuators A Phys 262:46–63
55. Black J, Stanier S, Clarke S (2009) Shear wave velocity measurement of Kaolin during undrained unconsolidated triaxial compression. InProceedings 62nd Can. Geotech. Conf., Sheffield:, p. 1–8
56. Airey D, Mohsin A (2013) Evaluation of shear wave velocity from bender elements using cross-correlation. Geotech Test J 36:506–514. https://doi.org/10.1520/GTJ20120125
57. Ogino T, Kawaguchi T, Yamashita S, Kawajiri S (2015) Measurement deviations for shear wave velocity of bender element test using time domain, cross-correlation, and frequency domain approaches. Soils Found 55:329–342
58. Ram AK, Mohanty S (2021) Experimental investigation on dynamic behavior of silt-rich fly ash using cyclic triaxial and bender element tests. Innov Infrastruct Solut 6:1–24. https://doi.org/10.1007/S41062-021-00582-1
59. Rawat P, Mohanty S (2023) Study on cyclic strength and pore water pressure response of fiber- reinforced municipal solid waste (MSW) fines. Acta Geotech 3:1–15. https://doi.org/10.1007/s11440-023-01818-3
60. Georgetti G, Vilar O, Rodrigues R (2013) Small-strain shear modulus and shear strength of an unsaturated clayey sand. InProceedings 18th Int. Conf. Soil Mech. Geotech. Eng, Paris, p. 1113–6
61. Heidarizadeh Y, Lajevardi SH, Sharifipour M (2021) Correlation between small-strain shear stiffness and compressive strength of clayey soils stabilized with cement and nano-SiO2. Int J Geosynth Gr Eng 7:1–12. https://doi.org/10.1007/S40891-021-00258-X

62. Donovan J, Marketos G, Sullivan C (2015) Novel methods of bender element test analysis. In: Soga K, Kumar K, Biscontin G, Kuo M, editors. Geomech. from Micro to Marco, London: Taylor and Francic, p. 311–6
63. Da FA, Ferreira C, Fahey M (2009) A framework interpreting bender element tests, combining time-domain and frequency-domain methods. Geotech Test J 32:91–107
64. Palczyńska A, Wymysłowski A, Bieniek T, Janczyk G, Pasquet D, Dinh T (2014) Crosstalk phenomena analysis using electromagnetic wave propagation by experimental an numerical simulation methods. 15th Int. Conf. Therm. Mech. Mulit-Physics Simul. Exp. Microelectron. Microsystems, p. 1–10
65. Li H, Senetakis K (2017) Dynamic properties of polypropylene fibre-reinforced silica quarry sand. Soil Dyn Earthq Eng 100:224–232
66. Claria J, Vettorelo P (2016) Mechanical behavior of loose sand reinforced with synthetic fibers. Soil Mech Found Eng 53:12–28

Springer Nature or its licensor (e.g. a society or other partner) holds exclusive rights to this article under a publishing agreement with the author(s) or other rightsholder(s); author self-archiving of the accepted manuscript version of this article is solely governed by the terms of such publishing agreement and applicable law.